DIRECT CONVERSION OF BIOMASS TO ELECTRICITY WITH SOLID OXIDE FUEL CELL TECHNOLOGY

Yusuke Shiratori[1,2], Quang-Tuyen Tran[1], and Kazunari Sasaki[1,2,3]

[1] Department of Mechanical Engineering, Faculty of Engineering, Kyushu University, Fukuoka, Japan, Tel: 81-92-802-3058, e-mail: y-shira@mech.kyushu-u.ac.jp

[2] International Institute for Carbon-Neutral Energy Research (WPI), Kyushu University, Fukuoka, Japan
[3]International Research Center for Hydrogen Energy, Kyushu University, Fukuoka, Japan

Abstract

Fuel cells are electrochemical devices that convert chemical energy of fuels directly into electrical energy without the Carnot limitation. Even in the smallest power range of less than 10 kW, fuel cells exhibit electrical efficiencies of 35-50 %LHV (lower heating value). Therefore, the fuel cell which can be operated with very low environmental emission levels, is regarded as a promising candidate for a distributed power source in the next generation. Although most fuel cells operate with hydrogen as a fuel, solid oxide fuel cells (SOFCs) operated in a high temperature range between 600 and 900ºC accept the direct use of hydrocarbon fuels. Recently, the present research have demonstrated the stable operation of a direct internal reforming SOFC (DIRSOFC) operating not only on non-synthetic biogas over one month using an anode-supported button cell but also on practical palm-biodiesel over 800 h. Here, performances of DIRSOFCs operating on biogas are summarized and roadblocks to overcome for the realization of this type of highly-efficient carbon-neutral fuel cell are discussed.

Keywords: Biogas, Carbon deposition, Direct internal reforming, Impurity poisoning, Solid oxide fuel cell, Temperature distribution

Introduction

Although most fuel cells operate with hydrogen as a fuel, solid oxide fuel cells (SOFCs) operated in a high temperature range between 600 and 900 ºC accept the direct use of hydrocarbon fuels. Hydrocarbon fuels directly supplied to SOFCs are reformed in the porous anode materials producing H_2-rich syngas, which is subsequently used to generate electricity and heat through electrochemical oxidation [1,2]. This type of SOFC, so called direct internal reforming SOFC (DIRSOFC), enables us to simplify the SOFC system. Electrochemical performances of DIRSOFC have been reported for gaseous and liquid fossil fuels such as methane [3], propane [4], n-dodecane [5], synthetic diesel [6], crude oil and jet fuel [7]. Highly efficient fuel cells operated by fossil fuels can certainly contribute to the suppression of environmentally harmful emissions, but in view of exhaustion of fossil resources, the utilization of renewable bio-energies should be more promoted. Direct feeding of biofuels to SOFC gives an environmental-friendly, compact and cost-effective energy conversion system. Biogas derived primarily from garbage is one of the most attractive bio-energies for SOFC [8-11]. Recently, Shiratori et al. [10] has demonstrated the stable operation of a DIRSOFC operating on non-synthetic biogas over one month using an anode-supported button cell. On the other hand, the use of liquid biofuels is also attractive due to their easy storage and transportation with high energy density. Tran et al. [12] has demonstrated the stable operation of a DIRSOFC operating on practical palm-

biodiesel over 800 h, also using an anode-supported button cell. In this paper, performances of DIRSOFCs operating on biogas are summarized and roadblocks to overcome for the realization of this type of highly-efficient carbon-neutral fuel cell are mentioned.

Solid Oxide Fuel Cell

Operation Mechanism of SOFC

A fuel cell in general converts chemical energy of the fuel directly into electrical energy without converting it to mechanical energy. Therefore, the fuel cell has potential of attaining higher electrical conversion efficiency than those of conventional technologies such as heat engines limited by Carnot efficiency. Figure 1 shows the principle of SOFC operation. The basic unit of an SOFC, i.e. cell, consists of an electrolyte sandwiched with two electrodes, anode and cathode. In the electricity generation process, an oxide ion O^{2-} is generated from oxygen in air via the cathodic reaction (1).

$$1/2O_2(g) + 2e^- \rightarrow O^{2-} \tag{1}$$

Normally, SOFCs are operated in the temperature range between 600 and 900 °C in which electrolytes composed of doped metal oxides can exhibit rather high oxygen ion conductivity. Oxygen ions generated in the cathode are transported to the anode side through the dense electrolyte and are used to electrochemically oxidize a fuel, here hydrogen, in the anodic reaction (2).

$$H_2(g) + O^{2-} \rightarrow H_2O(g) + 2e^- \tag{2}$$

$$CO(g) + O^{2-} \rightarrow CO_2(g) + 2e^- \tag{3}$$

In the high temperature SOFC, not only hydrogen but also carbon monoxide can contribute to the generation of electricity (3). Hydrogen and carbon monoxide can be produced by steam reforming or partial oxidation of hydrocarbon fuels on the Ni-based anode material, therefore in principle hydrocarbon fuels can be directly supplied to SOFC without using a pre-reformer.

The electromotive force of fuel cell, E, derived from the difference in the partial pressure of oxygen, $p(O_2)$, between cathode and anode sides can be expressed by the Nernst equation (4).

$$E = (RT/4F)\ln\{p(O_{2,c})/p(O_{2,a})\}, \tag{4}$$

where R is the gas constant, F is Faraday constant, and T is absolute temperature. a and c denote anode and cathode sides, respectively. Theoretically, E is approximately 1 volt, and the ideal electrical efficiency can be calculated by $\Delta G/\Delta H$, where ΔG and ΔH are Gibbs free energy change and enthalpy change of the hydrogen combustion reaction (5), respectively. At the operating temperature of 800 °C ideal efficiency becomes 70 %LHV.

$$H_2(g) + 1/2O_2(g) = H_2O(g) \tag{5}$$

The actual electrical efficiency of an SOFC (40-50 %LHV) is always lower than the ideal value because fuel utilization (U_f) cannot be increased up to 100 % in the practical SOFC system and the contribution of the internal resistances such as resistances of the materials themselves, contact resistances and electrode reaction resistances is not negligible. However, in the small size fuel cell systems, the heat generation, including the intrinsic heat release, $\Delta H - \Delta G$, can be utilized effectively on site leading to overall efficiency above 80 %LHV.

The SOFC has the following advantages because of its high operating temperature. Various kinds of fuel, such as natural gas, liquefied petroleum gas, kerosene and biofuels, etc. can be utilized with a simple fuel processing system. Even direct feeding of such practical fuels is theoretically possible. Higher electrical efficiency above 50 %LHV can be obtained by setting higher fuel utilization. Overall efficiency can be enhanced by using the heat released from the cell for the fuel reforming process, in which endothermic steam reforming proceeds as a main reaction. This kind of energy recycle is possible because the operational temperature of SOFC is nearly the same as that of the reformer. In addition, further enhancement of electrical efficiency is expected by using residual fuel and water vapor in a downstream gas turbine and steam turbine. High quality heat from the high temperature SOFC system can also be utilized effectively for hot water supply as well as reformer.
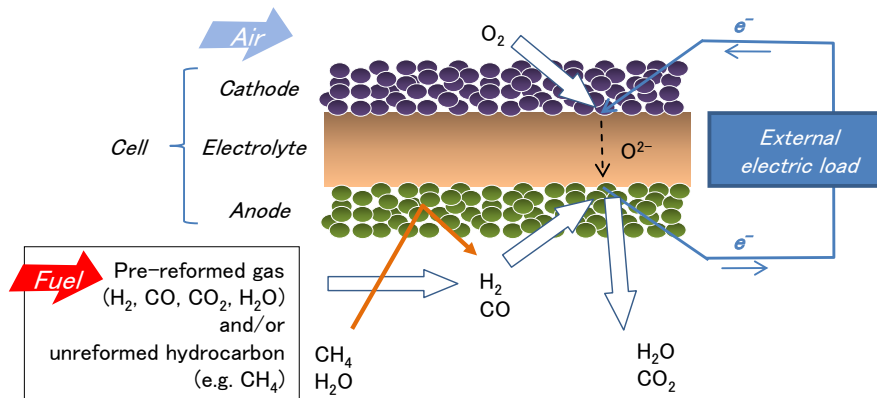

Figure 1. Principle of SOFC operation

Structure

In Table 1, requirements for component materials of a cell and interconnector are summarized. Typical materials are also listed in this table. The electrolyte has to be gas-tight to prevent leakage of fuel and oxidant gases. Both electrodes have to be porous to provide electrochemical reaction sites. The interconnector plays a role of electrically connecting the anode of one cell and the cathode of the adjoining cell, and also separating the fuel in the anode side from the oxidant in the cathode side. Component materials must be heat resistant and durable in the highly oxidative and reductive atmospheres for cathode and anode sides, respectively.

To fabricate a cell, powders of these component materials are formed into desired shapes by general ceramic processing such as extrusion, slip casting, pressing, tape casting, printing and dip coating [13]. Subsequently, the resulting "green" ceramics undergo heat-treatments. High temperature sintering processing above 1300 °C is normally required to obtain a dense and gas tight electrolyte layer.

In an SOFC, all solid state fuel cell, various types of cell configuration have been designed and classified by support materials and shapes. The SOFC has a laminate structure of thin ceramic layers, therefore a support material is necessary to ensure the mechanical stability. Anode-supported, electrolyte-supported, cathode-supported, metal-supported and nonconductive ceramic-supported (segmented-in-series) types have been developed. From the viewpoint of cell shape, there are roughly three types, i.e., planar, flat tubular and tubular types.

Table 1. Component Materials of SOFC

Component Materials		Requirements	Typical materials
Cell	Electrolyte	Dense (Gas tight), Ionically conductive	Y_2O_3-stabilized ZrO_2 (YSZ), Sc_2O_3-stabilized ZrO_2 (ScSZ), Gd_2O_3 doped CeO_2 (GDC), $(La,Sr)(Ga,Mg)O_3$ (LSGM))
	Anode	Porous, Electrochemically active, Electronically conductive	Ni-YSZ, Ni-ScSZ, Ni-GDC
	Cathode	Porous, Electrochemically active, Electronically conductive	$(La,Sr)MnO_3$, $(La,Sr)(Fe,Co)O_3$
Interconnector		Dense (Gas tight), Electronically conductive	$(La,Sr)CrO_3$, $(La,Ca)CrO_3$ $(Sr,La)TiO_3$, Stainless steel

Resistance of the electrolyte dominates the internal voltage loss in many cases, thus making thinner electrolytes is a key technology to achieve better performance especially at lower operating temperatures. For example, an anode-supported cell (Figure 2a), in which a thin electrolyte layer with a thickness of around 15 μm is formed on the anode substrate with a thickness of 1 mm, enables operation of an SOFC around 200 K lower in temperature as compared to an electrolyte-supported cell (Figure 2b) [1].
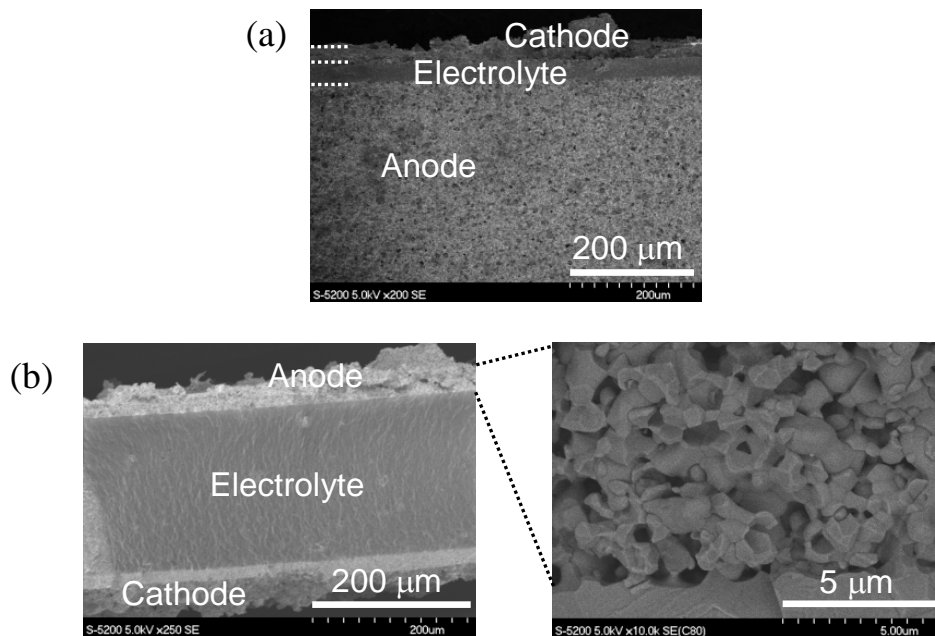

Figure 2. FESEM images of (a) anode-supported cell and (b) electrolyte-supported cell

Large scale SOFC systems are being developed aiming for a distributed electrical power plant with high energy conversion efficiency. Mitsubishi Heavy Industries (JP) has developed a 200 kW class micro gas turbine hybrid system as shown in Figure 3 with a maximum efficiency of 52.1% LHV, and a maximum gross power of 229 kW-AC was achieved with natural gas as a fuel. Their final goal is to achieve electrical efficiency of

70% by developing large-scale power generation system in which the SOFC integrates with gas turbines and steam turbines [14].

Small scale SOFCs of 1-2 kW class are now being developed all over the world, aiming at early commercialization of residential CHP systems. City gas is generally used as a fuel with high overall efficiency more than 80 %LHV obtained by utilizing both electricity and heat on site. In Japan, a demonstrative research project is now being carried out in which Kyocera (JP), Tokyo gas (JP) and TOTO (JP) participate as manufacturers of SOFC stacks. More than 200 systems have been installed on actual residential sites as of FY2010. In this project, reductions of primary energy consumption and CO_2 emission by 16 and 34 %, respectively, were demonstrated [15].
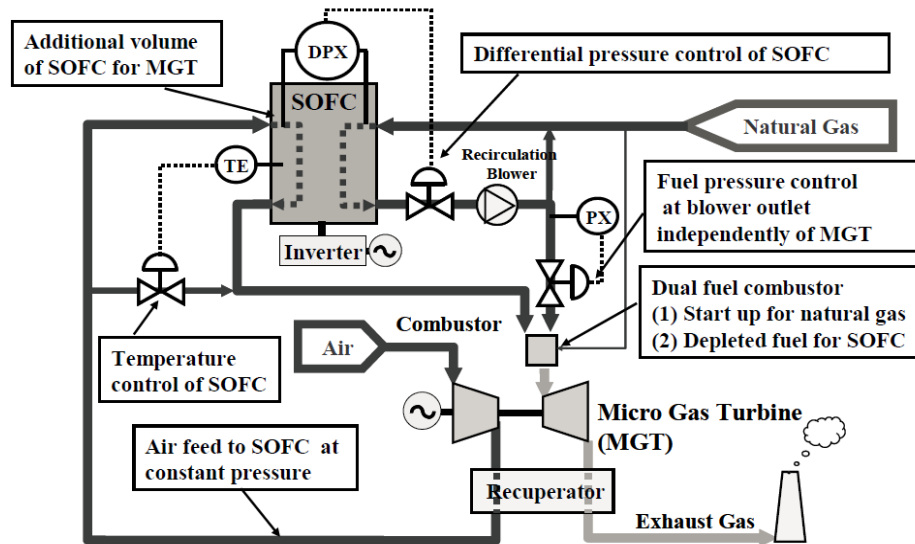

Figure 3. Flow diagram of 200 kW-class SOFC-micro gas turbine combined system developed by Mitsubishi Heavy Industries [14]

Experimental

SOFC Single Cell Used in the Tests

Ni-yttria stabilized zirconia cermet (Ni-YSZ) is the most popular material for SOFC anodes. However, it has been reported that Ni-scandia stabilized zirconia (Ni-ScSZ) offers better catalytic performance and can suppress coking when hydrocarbon fuels are supplied to SOFC [16]. Thus, we used anode-supported type cells based on the anode/electrolyte bi-layer (half-cell) of Ni-ScSZ/ScSZ to evaluate the electrochemical and catalytic performance of DIRSOFCs operating on biofuels. Two types of half cells, button cell with diameter of 20 mm and square-shaped cells with area of 5 x 5 cm^2 purchased from Japan fine ceramics were used to fabricate single cells. The cells consist of ScSZ electrolyte with a thickness of 14 μm sintered on a porous anode support (mixture of NiO and ScSZ (NiO:ScSZ = 5.6:4.4)) with a thickness of 800 μm. A mixture of $(La_{0.8}Sr_{0.2})_{0.98}MnO_3$ (> 99.9 %, Praxair, USA, abbreviated by LSM) and ScSZ (Daiichi Kigenso Kagaku Kogyo, Japan) with a weight ratio of 1:1 was adopted as a cathode functional layer and coarse LSM was applied as a cathode current collector layer. Porous cathodes with the area of 0.8 x 0.8 and 4 x 4 cm^2 for button and square-shaped cells, respectively, were obtained by sintering process at 1200 ℃ for 3 h. Component materials of the single cells were summarized in Table 2.

Table 2. Component Materials of the Anode-Supported Single Cells Used in this Study

Component Materials	Composition	Thickness / μm
Electrolyte	10 mol% Sc_2O_3-1 mol% CeO_2-ZrO_2 (ScSZ)	14
Anode functional layer	56%NiO-44%ScSZ	26
Anode substrate	56%NiO-44%ScSZ	800
Cathode	50%$(La_{0.8}Sr_{0.2})_{0.98}MnO_3$ (LSM)-50%ScSZ	~30
Cathode current collector layer	LSM	~30

Measurement of Temperature Distribution

SOFC visualization system was built and used to evaluate thermo-mechanical properties of DIRSOFC. In this experiment, square-shaped half cell (anode-supported type) with the area of 5 x 5 cm^2 was adopted and mounted in the special cell housing which can simulate a fuel flow of real SOFC systems. 100 ml min^{-1} of simulated biogas mixture (CH_4/CO_2 = 1.5) was fed into the porous anode material from one side to another side in-plane direction. Inside of the furnace was filled with still air maintained at 800 ^{o}C. Bi-dimensional temperature distribution of the surface of the half cell was monitored from the electrolyte side during the supply of simulated biogas by thermography (TVS8500, NEC Avio) with InSb FPA detector.

DIRSOFC Testing System

The SOFC testing system [10] and automatic gas chromatograph were connected to the methane fermentation reactor placed in Tosu Kankyo Kaihatsu Ltd. as shown in Figure 4. Garbage collected in Tosu-city of Saga prefecture was mixed with water resulting in waste slurry. After materials unsuitable for anaerobic fermentation were filtered out, cattle manure was added to the slurry followed by the treatment with acid and methane fermentation processes to produce biogas (mixture of CH_4 and CO_2) containing 790 ppm H_2S. The raw biogas was passed through a desulfurizer packed with FeO pellets 20 cm^3 in size. The typical composition of desulfurized biogas sampled from the fermentation reactor is listed in Table 3. The concentration of H_2S was less than 0.5 ppm. The concentrations of the other fuel impurities, CH_3SH, Cl_2, HCl, NH_3 and siloxane, were below the detection limits (2 ppb, 60 ppb, 0.4 ppm, 0.6 ppm and 10 ppb, respectively), indicating that this gas can be fed directly into a SOFC [17]. In any case, 1 ppm level H_2S contamination must be taken into account even after desulfurization treatment. The pressure controlled real biogas (0.1 MPa) was directly distributed to the SOFC at 800 ^{o}C and the gas chromatograph. The experimental setup for testing DIRSOFC operating on biogas has been described elsewhere [10].

Table 3. Typical Composition of the Actual Desulfurixed Biogas [10]

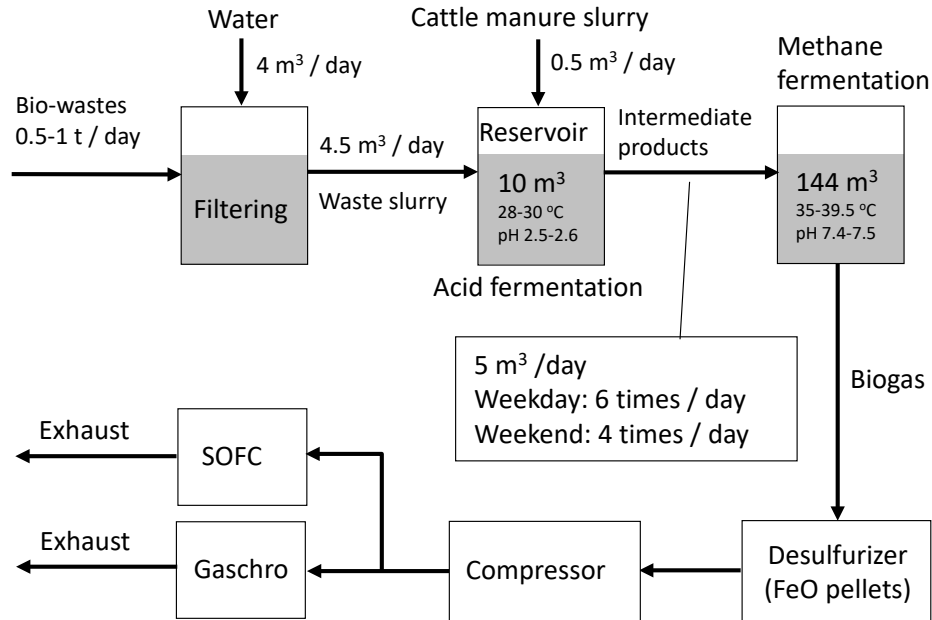| Gaseous Species	Concentration / Vol%
CH_4	62.6 vol %
CO_2	35.7 vol %
H_2O	1.62 vol %
N_2	0.09 vol %
H_2	99 vol ppm
H_2S	< 0.5 ppm

Figure 4. Connection of SOFC test system and gas chromatograph with the methane fermentation reactor in Tosu-city, Japan [10,11]

Results and Discussion

Long Term Test of DIRSOFC with Biogas

The main reactions involved in a DIRSOFC running on biogas are summarized here. Internal dry reforming of CH_4 (reaction 6) proceeds on a Ni-based anode using CO_2 inherently included in biogas without an external reformer. Then, the produced H_2 and CO are electrochemically oxidized to produce electricity (reactions (2) and (3)) [18].

$$CH_4 + CO_2 \rightarrow 2CO + 2H_2 \qquad\qquad (6)$$

Only a few reports have provided the performance of DIRSOFCs operating on biogas [9,10,19-21], because carbon formation thermodynamically can take place on the anode material. Staniforth et al. [19] has reported the results of direct-feeding of landfill biogas (general CH_4-rich biogas). However, that was a short term experiment and not continuous feeding of as-produced real biogas. To avoid coking, pre-reforming of biogas is generally required [22]. Recently, development of a new fermentation path producing H_2-rich biogas [23] and highly active catalysts to assist biofuel reforming [24-26] have been reported. Heretofore, we have succeeded in stable operation of a DIRSOFC running on actual biogas produced in waste treatment center using Ni-ScSZ cermet as an anode material without any support catalysts.

Figure 5a shows the cell voltages of DIRSOFC operating on biogas measured at 200 mA cm^{-2}. Simulated biogas with the CH_4/CO_2 ratio of 1.5 led to a stable cell voltage above 0.8 V for 800 h. The degradation rate of only 0.4 %/1000 h proved that the biogas-fueled SOFC can be operated with an internal reforming mode. For the real biogas generated from the methane fermentation reactor, rather high voltage comparable to that obtained by simulated biogas was achieved for 1 month, although there is a voltage fluctuation. Monitoring of biogas composition simultaneously with the cell voltage (Figure 5b) revealed that voltage fluctuation (a maximum of 50 mV level) appeared in synchronization

with the fluctuation of CH_4/CO_2 ratio. An abrupt increase in CO_2 concentration induced temporarily decreased cell voltage. The CH_4/CO_2 ratio in the real biogas fluctuated between 1.4 and 1.7 which corresponds to CH_4 concentration range between 58 and 63 vol%. The biogas composition is influenced by many factors, for example, type of organic wastes, physical states and operational conditions of methane fermentation such as temperature and pH of the waste slurry.
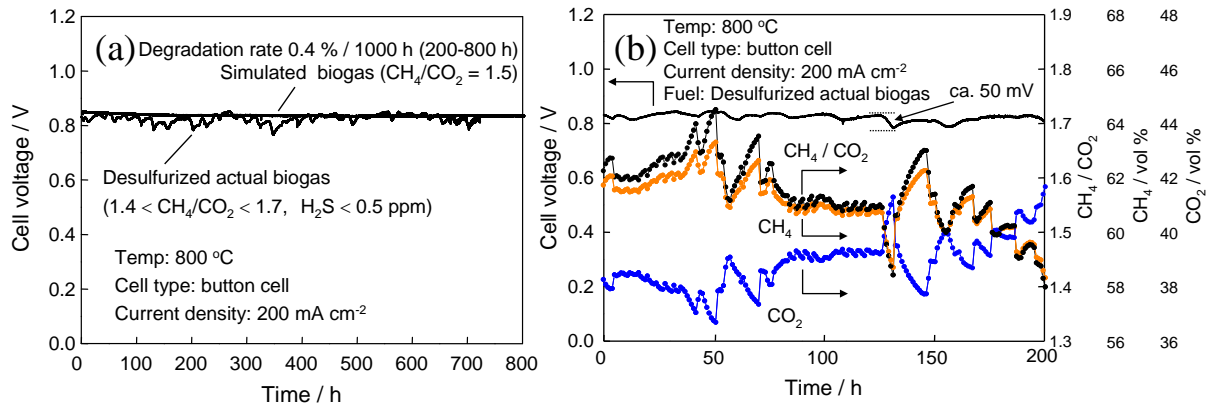

Figure 5. Performance of DIRSOFC operating on biogas [18]; (a) the results measured at 800 oC using anode-supported button cells and (b) voltage fluctuation in synchronization with the fluctuation of biogas composition during the long term test (initial 200 h of (a))

From the thermodynamic point of view, a CH_4/CO_2 ratio of 1.5 should cause coking at 800 °C, however carbon formation did not occur on the anode support for simulated biogas even after 800 h as shown in Fig. 6a. Provided that a fuel cell current is applied, this fuel composition close to the border of the carbon deposition region may not cause coking [10]. As for the real biogas, severe coking occurred during the long term test (Figure 6b). The trigger of the coking was trace H_2S (< 0.5 ppm) in the real biogas which can cause deactivation of Ni catalyst for the dry reforming of methane [9,27]. Although a threshold of maximum H_2S concentration tolerance for Ni-stabilized zirconia cermet anode must be provided in future work, total sulfur concentration should be reduced to less than 0.5 ppm level by employing an optimum desulfurization process.
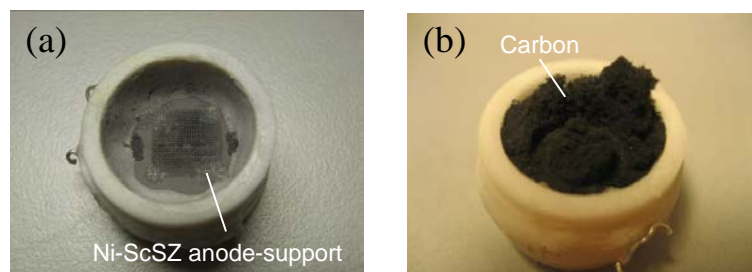

Figure 6. Anode-supported cells after long term test shown in Fig. 5a using (a) simulated and (b) practical biogases

Problems to be Solved for the Realization of DIRSOFC Running on Biogas

Impurity Poisoning

Generally biofuels including biogas and BDFs contain several kinds of impurities such as sulfur compounds. According to thermochemical calculations [17], sulfur compounds exist as H_2S at SOFC operational temperatures in equilibrium. Here, in order to investigate the influence of a fuel impurity, 1 ppm H_2S was mixed with simulated biogas mixture

($CH_4/CO_2 = 1.5$) during the galvanostatic measurement under 200 mA cm^{-2}. CO yield and selectivity were measured simultaneously with the electrochemical measurements. CO yield and selectivity are defined as

$$CO \text{ yield} = vCO / (fCH_4 + fCO_2) \quad (7)$$
$$CO \text{ selectivity} = vCO / (vCH_4 + vCO_2) \quad (8)$$

where vCO is CO formation rate, and fCH_4 and fCO_2 are feeding rates of CH_4 and CO_2, respectively, and vCH_4 and vCO_2 are consumption rates of CH_4 and CO_2, respectively. vCO, vCH_4 and vCO_2 were estimated from the results of the exhaust gas analysis. The results of H_2S poisoning test at 1000 °C are summarized in Figure 7.

In this experiment, an electrolyte-supported cell was used to measure anodic overvoltage separately from cathodic overvoltage using a Pt reference electrode [9]. The horizontal axis indicates the time after starting poisoning. As shown in Figure 7a even if 1 ppm H_2S was included in biogas, a cell voltage of about 1 V was stable during 20 h operation while voltage drop of about 100 mV (9 % of initial cell voltage) occurred in the first 1 h. The voltage drop was caused by increase in anodic overvoltage. Just after starting 1 ppm H_2S poisoning, anodic overvoltage grew to be 3.6 times larger compared to the initial value, which would be due to sulfur surface coverage of Ni catalysts. On the other hand, the anode-side IR drop did not change by the H_2S poisoning.
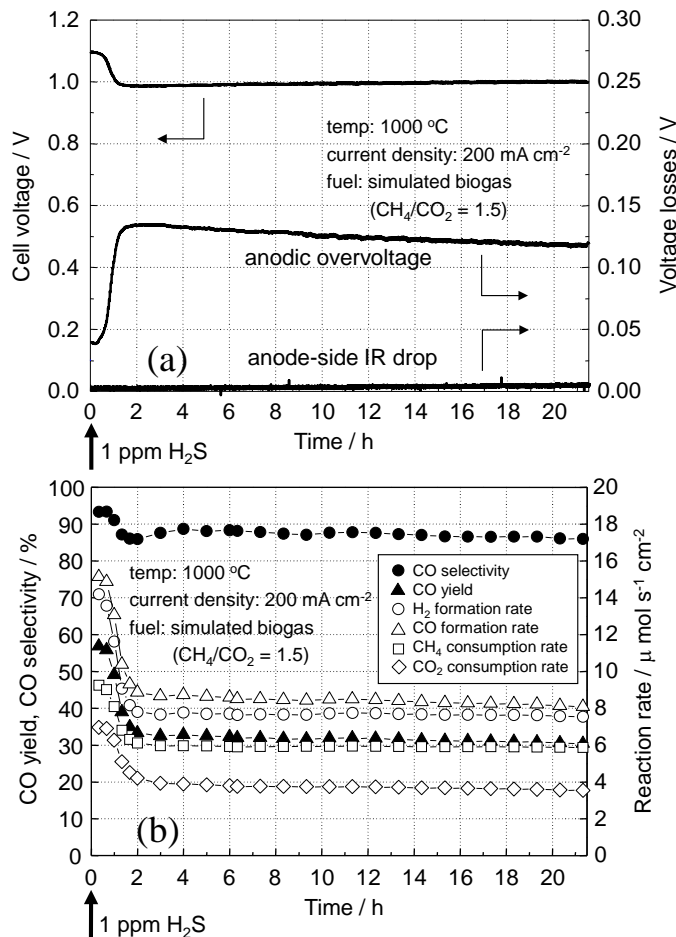

Figure 7. Electrochemical and catalytic performance of Ni-ScSZ anode during 1 ppm H_2S poisoning measured at 1000 °C under 200 mA cm^{-2}; (a) cell voltage, anodic overvoltage (IR free) and anode-side IR drop and (b) reaction rates, CO yield and CO selectivity for internal dry reforming of methane. Simulated biogas mixture, $CH_4/CO_2 = 1.5$, was fed as a fuel [9]

The reaction rates of internal reforming, CO yield and CO selectivity during 1 ppm H_2S poisoning test are plotted on Figure 7b. Rapid deactivation of the reforming reaction was observed within 2 h after starting H_2S poisoning resulting in about a 40 % decrease in reaction rates and CO yield. On the other hand, CO selectivity was less sensitive to H_2S contamination (only 7 % decrease). After the initial deactivation of the catalytic activity, a quasi-stable state appeared. Figure 8 schematically depicts the degradation mechanism of a DIRSOFC operating on biogas under H_2S contamination. Sulfur species chemisorbed on Ni catalyst not only deactivate reforming reaction but also block the triple phase boundary (TPB) which is the active reaction region for electrochemical oxidation of produced H_2 and CO. Deactivation of reforming reaction causes deficiency of H_2 and CO, and blockage of TPB sites causes an increase in local current density. These phenomena would appear as an initial increase in anodic overvoltage (or initial voltage drop). Cell voltage, CO yield and CO selectivity completely recovered within 4h after stopping H_2S poisoning, indicating that H_2S poisoning caused by adsorption of sulfur species is a reversible process and 1 ppm level H_2S contamination is not fatal for the operation of DIRSOFC running on biogas at 1000 °C.
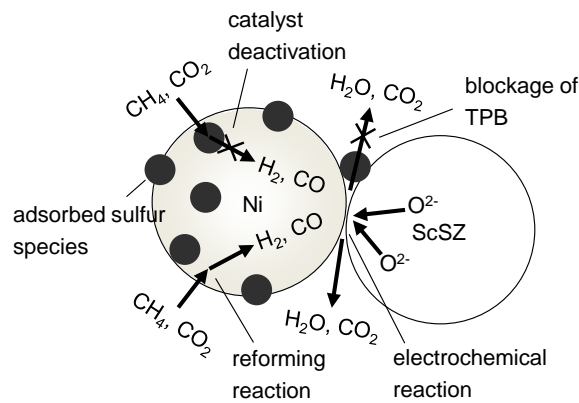

Figure 8. Possible degradation mechanism of DIRSOFC operating on biogas caused by H_2S contamination of biogas [9]

On the contrary, at 800 °C, 1 ppm H_2S was more detrimental. Cell voltage and internal reforming rates kept on decreasing during 22 h of H_2S poisoning. Voltage drop of about 170 mV (20 % of initial cell voltage) and 80 % decrease in the reaction rates occurred without the quasi-stable state as in the case of 1000 °C testing. The results summarized in Table 4 indicate that higher-grade desulfurization is required for lower operating temperatures, suggesting that the effect of impurity poisoning will become more detrimental at the cooled area in the cell.

Table 4. Impact of 1 ppm H_2S Contamination of Biogas on the Performance of DIRSOFC Running on Biogas Deduced by the 22 h Poisoning Test. Fuel: Simulated Biogas Mixture ($CH_4/CO_2 = 1.5$), Cell: Ni-ScSZ/ScSZ/LSM-ScSZ [18]

Temperature	Cell voltage	IR loss	Syngas Production	Degradation Behavior
1000 °C (Electrolyte-supported)	9 % decrease (100 mV)	no change	40 % decrease	initial voltage drop followed by quasi-stable state
800 °C (Anode-supported)	20 % decrease (170 mV)	no change	80 % decrease	continuous degradation

Strong Temperature Gradient

Ni-ScSZ/ScSZ/LSM-ScSZ square-shaped cells with an area of 25 cm^2 simulating a real SOFC were used for the evaluation of thermomechanical reliability of a DIRSOFC. When the simulated biogas (CH$_4$/CO$_2$ = 1.5) was directly fed to the square-shaped cell, long term operation could not be performed at 800 ºC [11]. This is due to a locally-decreased cell temperature caused by the strong endothermicity of internal reforming.
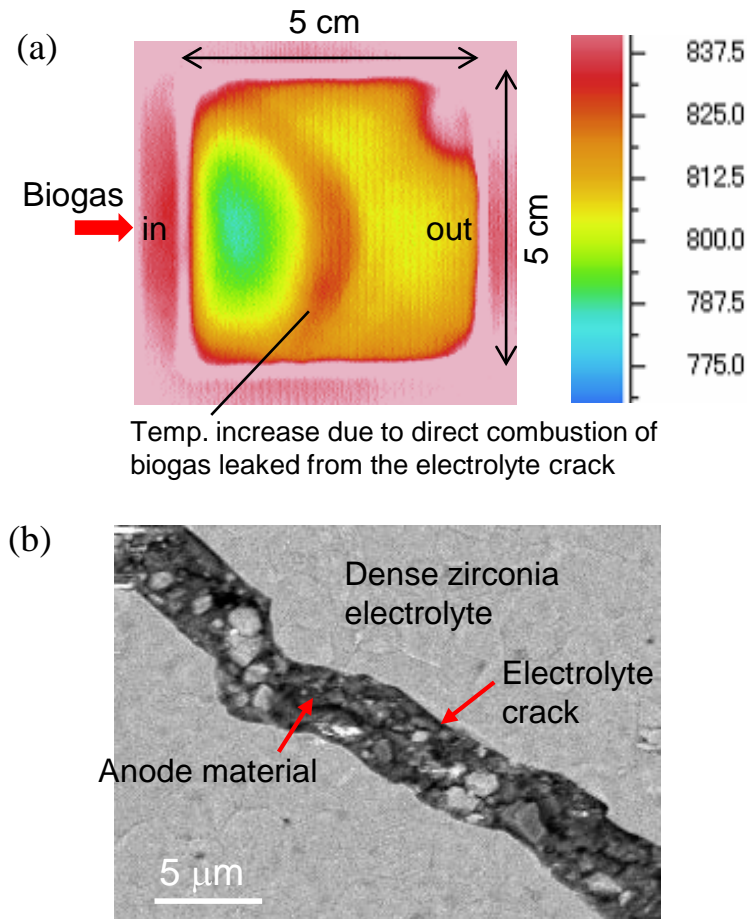

Figure 9. (a) The temperature distribution caused by internal dry reforming of methane and (b) resulting cell fracture observed along the edge of the cooled area shown in (a) detected by FESEM, showing brittleness of electrolyte thin film sintered on the anode support versus hydrocarbon fuel

To estimate the endothermicity of reaction (6), an equimolar mixture of CH$_4$ and CO$_2$ was supplied to the square-shaped anode-supported half-cell, and the temperature distribution generated in the half cell was measured from the electrolyte side by thermography. As shown in Figure 9a, a large temperature gradient was generated at the fuel inlet side, and the temperature around the cooled area considerably increased within 20 min, indicating the formation of an electrolyte crack (Figure 9b) from which biogas leaked and burned. When simulated biogas with CH$_4$/CO$_2$ = 1.5 was used as a fuel, at a furnace temperature of 800 ºC, as shown in Figure 10a, a strong temperature gradient formed in the half cell and led to an electrolyte crack within 15 min after starting the supply of simulated biogas. The temperature gradient became more moderate with air addition to the biogas, as can be seen in Figure 10b and c, for air/biogas of 1.0 and 1.5, respectively, at the same furnace temperature.
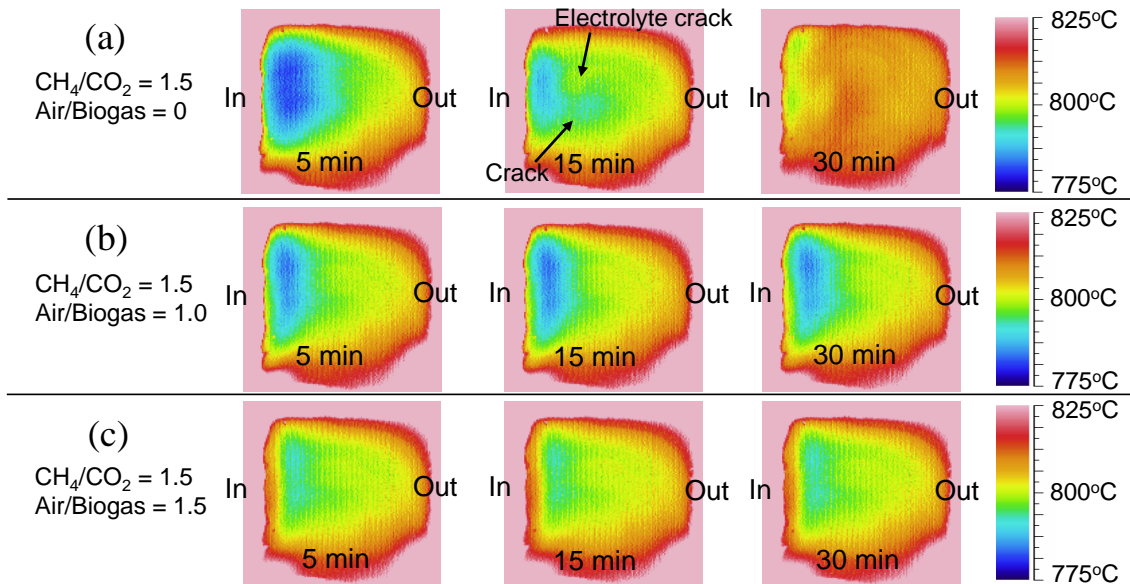
Figure 10. The temperature distribution in the Ni-ScSZ anode support when simulated biogases with $CH_4/CO_2 = 1.5$ were fed directly with a furnace temperature of 800 $^{\circ}$C under open circuit condition; (a) Air/Biogas =0, (b) 1.0 and (c) 1.5

Conclusions

In the course of this study, roadblocks for the realization of a direct internal reforming SOFC (DIRSOFC) operating on biofuels, which is promising candidate for a distributed generator in a coming carbon-neutral society, were uncovered. Simulated biogas with the CH_4/CO_2 ratio of 1.5 led to a stable cell voltage above 0.8 V for 800 h. The degradation rate of only 0.4 %/1000 h proved that the biogas-fueled SOFC can be operated with an internal reforming mode. As for the real biogas, severe coking occurred during the long term test. The trigger of the coking was trace H_2S (< 0.5 ppm) in the real biogas which can cause deactivation of Ni catalyst for the dry reforming of methane. Sulfur species chemisorbed on Ni catalyst not only deactivate reforming reaction but also block the active reaction region for electrochemical oxidation of produced H_2 and CO. These phenomena would appear as an increase in anodic overvoltage. The higher-grade desulfurization is required for lower operating temperatures. In the internal reforming operation of real SOFC, stress concentration caused by the endothermic reforming reaction would take place along the cooled area near the fuel inlet. The internal stress may cause cracks or destruction of the electrolyte. Air addition to biogas was effective not only to avoid coking but also to suppress the steep temperature gradient because of the occurrence of exothermic reactions (partial and complete oxidation of methane). Although the feasibility of a DIRSOFC running on biogas has been demonstrated, there is an urgent need to collect more practical data using a real stack.

Acknowledgements

References

[1] B.C.H. Steele, and A. Heinzel, "Materials for fuel-cell technologies," *Nature*, Vol. 414, pp. 345-352, 2001.

[2] K. Sasaki, and Y. Teraoka, "Equilibria in fuel cell gases: I. equilibrium compositions and reforming conditions," *Journal of Electrochemical Society*, Vol. 150 No. 7, pp. A878-A884, 2003.

[3] S. Park, R. Cracium, J.M. Vohs, and R.J. Gorte, "Direct oxidation of hydrocarbons in a solid oxide fuel cell: I. methane oxidation," *Journal of Electrochemical Society*, Vol. 146, No. 10, pp. 3603-3605, 1999.

[4] T. Iida, M. Kawano, T. Matsui, R. Kikuchi, and K. Eguchi, "Internal reforming of SOFCs: Carbon deposition on fuel electrode and subsequent deterioration of cell," *Journal of Electrochemical Society*, Vol. 154, No. 2, pp. B234-B241, 2007.

[5] H. Kishimoto, K. Yamaji, T. Horita, Y. Xiong, N. Sakai, M. Brito, and H. Yokokawa, "Feasibility of liquid hydrocarbon fuels for SOFC with Ni-ScSZ anode," *Journal of Power Sources*, Vol. 172, pp. 67-71, 2007.

[6] H. Kim, S. Park, J.M. Vohs, and R.J. Gorte, "Direct oxidation of liquid fuels in a solid oxide fuel cell," *Journal of Electrochemical Society*, Vol. 148, No. 7, pp. A693-A695, 2001.

[7] Z.F. Zhou, C. Gallo, M.B. Pargue, H. Schobert, and S.N. Lvov, "Direct oxidation of jet fuels and pennsylvania crude oil in a solid oxide fuel cell," *Journal of Power Sources*, Vol. 133, pp. 181-187, 2004.

[8] J. Van herle, Y. Membrez, and O. Bucheli, "Biogas as a fuel source for SOFC co-generators," *Journal of Power Sources*, Vol. 127, pp. 300-312, 2004.

[9] Y. Shiratori, T. Oshima, and K. Sasaki, "Feasibility of direct-biogas SOFC," *International Journal of Hydrogen Energy*, Vol. 33, pp. 6316-6321, 2008.

[10] Y. Shiratori, T. Ijichi, T. Oshima, and K. Sasaki, "Internal reforming SOFC running on biogas," *International Journal of Hydrogen Energy*, Vol. 35, pp. 7905-7912, 2010.

[11] Y. Shiratori, T. Ijichi, T. Oshima, and K. Sasaki, "Performance of internal reforming SOFC running on biogas," In: *9th European SOFC Forum, European Fuel Cell Forum Proceedings Series*, pp. 4-77-4-87, June 2010.

[12] Q.T. Tran, Y. Shiratori, and K. Sasaki, "Feasibility of palm-biodiesel fuel for internal reforming Solid Oxide Fuel Cells," *International Journal of Energy Research*, 2012, DOI: 10.1002/er.2883.

[13] D. Stöver, H.P. Buchkremer, and J.P.P. Huijsmans, "MEA/cell preparation methods: Europe/USA," In *Handbook of Fuel Cells-Fundamentals, Technology and Applications*, W. Vielstich, A. Lamm, and H.A. Gasteiger, eds.: John Wiley & Sons Ltd., pp. 1015-1031, 2003.

[14] S. Yoshida, T. Kabata, M. Nishiura, S. Koga, K. Tomida, K. Miyamoto, Y. Teramoto, N. Matake, H. Tsukuda, S. Suemori, Y. Ando, and Y. Kobayashi, "Development of the SOFC-GT combined cycle system with tubular type cell stack," *ECS Transactions*, Vol. 35 No. 1, pp. 105-111, 2011.

[15] K. Hosoi, M. Ito, and M. Fukae, "Status of national project for SOFC development in Japan," *ECS Transactions*, Vol. 35, No. 1, pp. 11-18, 2011.

[16] K. Ke, A. Gunji, H. Mori, S. Tsuchida, H. Takahashi, K. Ukai, Y. Mizutani, H. Sumi, M. Yokoyama, and K. Waki, "Effect of oxide on carbon deposition behavior of CH_4 fuel on Ni/ScSZ cermet anode in high temperature SOFCs," *Solid State Ionics*, Vol. 177, pp. 541–547, 2007.

[17] K. Haga, S. Adachi, Y. Shiratori, K. Itoh, and K. Sasaki, "Poisoning of SOFC anodes by various fuel impurities," *Solid State Ionics*, Vol. 179, pp. 1427-1431, 2008.

[18] Y. Shiratori, T. Ijichi, T. Oshima, and K. Sasaki, "Generation of electricity from organic bio-wastes using Solid Oxide Fuel Cell," *ECS Transactions*, Vol. 25, No. 2, pp. 1051-1060, 2009.

[19] J. Staniforth, and K. Kendall, "Cannock landfill gas powering a small tubular solid oxide fuel cell - A case study," *Journal of Power Sources*, Vol. 86, pp. 401-403, 2000.

[20] K. Girona, J. Laurencin, M. Petitjean, J. Fouletier, and F. Lefebvre-Joud, "SOFC running on biogas: Identification and experimental validation of 'Safe' operating conditions," *ECS Transactions*, Vol. 25, No. 2, pp. 1041-1050, 2009.

[21] A. Lanzini, and P. Leone, "Experimental investigation of direct internal reforming of biogas in solid oxide fuel cells," *International Journal of Hydrogen Energy*, Vol. 35, pp. 2463-2476, 2010.

[22] J. Van Herle, F. Maréchal, S. Leuenberger, Y. Membrez, O. Bucheli, and D. Favrat, "Process flow model of solid oxide fuel cell system supplied with sewage biogas," *Journal of Power Sources*, Vol. 131, pp. 127-141, 2004.

[23] P. Leone, A. Lanzini, M. Santarelli, M. Cali, F. Sagnelli, A. Boulanger, A. Scaletta, and P. Zitella, "Methane-free biogas for direct feeding of solid oxide fuel cells," *Journal of Power Sources*, Vol. 195, pp. 239-248, 2010.

[24] J. Xuan, M.K.H. Leung, D.Y.C. Leung, and M. Ni, "A review of biomass-derived fuel processors for fuel cell systems," *Renewable and Sustainable Energy Reviews*, Vol. 13, pp. 1301-1313, 2009.

[25] I.V. Yentekakis, "Open- and closed-circuit study of an intermediate temperature SOFC directly fueled with simulated biogas mixtures," *Journal of Power Sources*, Vol. 160, pp. 422–425, 2006.

[26] Z.F. Zhou, R. Kumar, S.T. Thakur, L.R. Rudnick, H. Schobert, and S.N. Lvov, "Direct oxidation of waste vegetable oil in solid-oxide fuel cells," *Journal of Power Sources*, Vol. 171, pp. 856-860, 2007.

[27] K. Sasaki, K. Haga, T. Yoshizumi, D. Minematsu, E. Yuki, R.R. Liu, C. Uryu, T. Oshima, S. Taniguchi, Y. Shiratori, and K. Ito, "Impurity poisoning of SOFCs," *ECS Transactions*, Vol. 35, No. 1, pp. 2805-2814, 2011.